Development 137, 4039-4049 (2010) doi:10.1242/dev.055269

Spiralian quartet developmental potential is regulated by specific localization elements that mediate asymmetric RNA segregation

Jeremy S. Rabinowitz and J. David Lambert*

SUMMARY

Spiralian embryos are found in a large group of invertebrate phyla but are largely uncharacterized at a molecular level. These embryos are thought to be particularly reliant on autonomous cues for patterning, and thus represent potentially useful models for understanding asymmetric cell division. The series of asymmetric divisions that produce the micromere quartets are particularly important for patterning because they subdivide the animal-vegetal axis into tiers of cells with different developmental potentials. In the embryo of the snail *Ilyanassa*, the IoLR5 RNA is specifically segregated to the first quartet cells during the third cleavage. Here, we show that this RNA, and later the protein, are maintained in the $1q^{121}$ cells and their descendents throughout development. Some IoLR5-expressing cells become internalized and join the developing cerebral ganglia. Knockdown of IoLR5 protein results in loss of the larval eyes, which normally develop in association with these ganglia. Segregation of this RNA to the first quartet cells does not occur if centrosomal localization is bypassed. We show that the specific inheritance of the RNA by the first quartet cells is driven by a discrete RNA sequence in the 3′ UTR that is necessary and sufficient for localization and segregation, and that localization of another RNA to the first quartet is mediated by a similar element. These results demonstrate that micromere quartet identity, a hallmark of the ancient spiralian developmental program, is controlled in part by specific RNA localization motifs.

KEY WORDS: RNA segregation, Asymmetric RNA localization, Centrosome, Spiralian

INTRODUCTION

Spiralian embryogenesis is defined by the characteristic asymmetry and chiral geometry of the early cell divisions (see Fig. 1). It is also distinguished by similarities in the fate maps of the blastulae produced by these divisions, even across long phylogenetic distances (Henry and Martindale, 1999; Lambert, 2010). Spiralian development is found in several phyla in the large clade of bilateral animals called the Lophotrochozoa. These include the annelids, molluscs, nemerteans, sipunculans and platyhelminthe flatworms. Recent phylogenetic evidence suggests that the last common ancestor of the Lophotrochozoa had spiral cleavage (Dunn et al., 2008), raising the possibility that the taxon Lophotrochozoa should revert to the earlier taxonomic term Spiralia (Schleip, 1929). These results indicate that spiralian development was present in the stem group of one of the three great clades of bilateral animals. This highlights the importance of understanding spiralian development for reconstructing the early evolution of development in protostomes and, by extension, in the bilateral metazoans.

The strong conservation of the cleavage pattern and fate map in these embryos allows homologous cells to be identified in distantly related groups. One of the hallmarks of spiralian development is the regionalization of the animal-vegetal axis by the production of three micromere quartets. The first two cleavages divide the embryo into four macromeres. The micromeres are produced when the four macromeres divide synchronously towards the animal pole in three successive divisions, producing the first, second and third quartet micromeres (Fig. 1A). Fate-mapping experiments have shown that across spiralian phyla, each quartet generates similar sets of fates (Ackermann et al., 2005; Boyer et al., 1996; Damen and Dictus, 1994; Hejnol et al., 2007; Henry and Martindale, 1998; Henry et al., 2004; Huang et al., 2002; Maslakova et al., 2004; Render, 1997; Weisblat and Shankland, 1985). Typically, the first quartet gives rise to the head ectoderm, including neural structures such as eyes, as well as to the majority of the primary ciliated band. For instance, in molluscs, the first quartet cells generate the ciliated lobes of the head (the velum), as well as anterior neural structures including the eyes (Fig. 1B). The second quartet usually gives rise to a posterior portion of the ciliated band and trunk ectoderm, whereas the third quartet normally generates ventral structures and foregut. Most of the mesoderm, including the heart and larval retractor muscle, is derived from the 4d cell, the fourth micromere formed by the D macromere.

Embryological experiments in *Ilyanassa* indicate that each quartet is born with a distinct developmental potential (Sweet, 1998). After transplantation, members of the first, but not the second, quartet can develop into eyes, consistent with the normal fate of the first quartet. Conversely, second, but not first, quartet cells can produce shell material. These landmark experiments showed that the spiralian micromeres acquire quartet-specific developmental potentials at, or shortly after, birth, but the molecular basis of this is not known. In the spiralian *Platynereis dumerilii*, asymmetries in the levels of nuclear β-catenin are required in different quartets for normal development. However, this appears to be a general property of divisions in the early embryo and does not provide quartet-specific cues (Schneider and Bowerman, 2007). In *Ilyanassa*, a number of quartet-specific RNAs have been discovered (Kingsley et al., 2007; Lambert and

Department of Biology, University of Rochester, Rochester, NY 14627, USA.

*Author for correspondence (dlamber2@mail.rochester.edu)

Accepted 29 September 2010

Nagy, 2002). In all cases examined thus far, these RNAs are inherited in a quartet-specific manner after first localizing to macromere centrosomes (Fig. 1A). These observations suggest that segregated RNAs might be involved in quartet-specific developmental potential, although none of these RNAs has been functionally implicated in development and the mechanisms that restrict them to particular cells are not known.

The present study focuses on the first quartet micromeres in *Ilyanassa*. First, we show that a particular RNA that is segregated to the first quartet, IoLR5, is required for the normal development of structures derived from this group of cells, i.e. the velum and the eyes (Clement, 1967; Render, 1991). Then, we define a narrow interval when centrosomal localization of RNA can occur, and show that this event is necessary for segregation to the first quartet. Finally, we identify a discrete secondary structure in the IoLR5 RNA that mediates localization to the centrosome and segregation to the first quartet. Our characterization of this structure and a similar one from another first quartet RNA suggests a model for how first quartet specificity is achieved.

MATERIALS AND METHODS

Animal collection and care

Adult *Ilyanassa obsoleta* were collected from the Bass River on Cape Cod, MA, the Peconic Bay in Riverhead, NY, Ocean Isle Beach, NC, or ordered from the Marine Resources Center at the Marine Biological Labs in Woods Hole, MA, USA. Animal care and embryo collection have been described (Collier, 1981; Gharbiah et al., 2009).

IoLR5 cloning

The IoLR5 clone isolated from a previously described in situ screen was 2055 bp (Kingsley et al., 2007). Northern blots on RNA from many individuals identified two transcripts of ~3.5 and ~3.0 kb. 3′ rapid amplification of cDNA ends (RACE) on a cDNA pool primed from a ligated linker generated an additional 1395 bp; 5′ ligation-mediated RACE yielded no additional bases. The new 3′ fragment contains a large microsatellite (~850 bp in the allele recovered in the 3′ RACE), which appears to be a continuous $(TC)_n$ repeat; we sequenced 100 bp of repeat from either side before the signal deteriorated, and we were unable to cut this region using a mixture of four four-cutter restriction enzymes that would be likely to cut if there were any significant length of non-repeat sequence in the region. PCR was performed on genomic DNA from many individuals, using primers flanking the microsatellite, resulting in bands of ~850 and ~400 bp. Consequently, the final clone is ~3450 bp (EU087578.1) and the 3.0 kb band seen on the northern blot is likely to be due to allelic variation in the microsatellite. We have identified a single intron using genomic PCR with primers along the transcript, but we have no evidence for alternatively spliced transcripts. We made a morpholino-resistant IoLR5 construct (IoLR5MOres) using fusion PCR (Szewczyk et al., 2006) to alter seven nucleotides in the morpholino binding site. IoTis11+IoLR5LE was made by inserting IoLR5LE at base-pair 47 in the original IoTis11 cDNA clone.

Antibody development and validation

We raised rabbit antibodies against a synthetic peptide corresponding to part of the IoLR5 protein (QMRMRERNYRVG) (Pocono Rabbit Farm and Laboratory, Canadensis, PA, USA). On western blots of *Ilyanassa* total protein, the affinity-purified antibody (at 1:1000 dilution) recognized two distinct bands at ~12 kDa and ~14 kDa, close to the 9.6 kDa predicted size of the IoLR5 protein. When animals were injected with IoLR5MO1, both bands on the western blot were diminished in strength, as was staining in whole-mount embryos.

In situ hybridization and antibody staining

Embryos were fixed and processed for in situ hybridization as previously described (Kingsley et al., 2007). Antibody staining and counterstaining with DAPI and phalloidin-Alexa Fluor 488 (Molecular Probes) were carried out as described (Lambert and Nagy, 2001) using a 1:800 dilution of the affinity-purified IoLR5 antibody.

IoLR5 knockdowns and scoring

Zygotes were injected with the indicated concentration of IoLR5MO1 (5′-GCTGGTGATACAACTCTTGATGACA-3′) or the Standard Control MO (5′-TATAAATTGTAACTGAGGTAAGAGG-3′) (Gene Tools), as previously described (Gharbiah et al., 2009; Rabinowitz et al., 2008). Embryos were reared for 7-15 days in 22 μM-filtered artificial seawater (FASW; Instant Ocean), then anesthetized and fixed as described (Lambert and Nagy, 2001). Larvae were individually scored at 400× with a Zeiss Axioplan 2 microscope. Capped and tailed IoLR5MOres mRNA was generated with the mScript Kit (Epicenter) and co-injected with IoLR5MO1 at ~450 ng/μl. For each manipulation, at least five embryos were scored from each of three or more different capsules to control for between-capsule variation.

RNA transcription, labeling and imaging

For localization element (LE) mapping experiments, fragments were amplified by PCR using a forward primer incorporating a T3 RNA polymerase site. DNA templates were phenol/chloroform extracted and ethanol precipitated before in vitro transcription with either digoxigenin-11-UTP (Roche) or ChromaTide Alexa Fluor 488-5-UTP (Molecular Probes) for 2-4 hours. Transcribed RNAs were treated with DNase I (Roche) for 20 minutes and those longer than 500 bases were purified using the MEGAclear Kit (Ambion), whereas those shorter than 500 bases were precipitated with sodium acetate and ethanol. Bright-field images were taken on a Zeiss Axioplan 2 microscope with a Canon 300D digital SLR camera and Qioptiq coupler (Fairport). Fluorescently labeled RNAs were imaged with a Leica SP5 confocal microscope and *z*-stacks were projected using Leica software.

We used the standard ratio of labeled to unlabeled nucleotide (1:3) for the digoxigenin-labeled RNAs, but we did not observe localization of Alexa Fluor 488-labeled RNAs unless we used a ratio of 1:12.5. This might be due to the fluorescent label interfering with the proper secondary structure of the LEs or with protein interactions. We could not detect the localization of fluorescent transcripts that were shorter than 500 bases, probably because of the low incorporation of label. At the 4-, 8- and 24-cell stages, the fluorescently labeled RNAs we tested had the same localization pattern as digoxigenin-labeled transcripts. At the 2-cell stage, only fluorescently labeled transcripts localized to centrosomes.

Morpholino inhibition of centrosomal transport

Capsules were divided so that half of the zygotes were injected with 1.0 mM IoLR5StemBlockMO (5′-CACTGTCCCCTCTAGGCAACATAGG-3′) and 1% Oregon Green 488 70,000 MW lysine-fixable dextran (Invitrogen) and the other half were injected with 1.0 mM IoLR5MO1 and 100 μM Sulforhodamine 101 (Invitrogen). Embryos were then pooled for fixation and in situ hybridization, following which the two sets could be distinguished by the presence of red versus green fluorescence from the co-injection solutions. Co-processing allowed for qualitative comparison between the two pools. Other experiments showed that Oregon Green dextran does not affect centrosomal localization of the endogenous RNA.

RESULTS

Characterization of the IoLR5 mRNA

A cDNA clone named IoLR5 (*Ilyanassa obsoleta* localized RNA 5) was recovered during a screen for localized RNAs during early cleavage stages (Kingsley et al., 2007). Northern blot hybridization identified transcripts of ~3.5 and ~3.0 kb (Fig. 1C). Using RACE PCR we extended the original 2055 bp IoLR5 cDNA to 3.5 kb (Fig. 1D). The two bands on the northern blot appear to be due to allelic size variation in a microsatellite (see Materials and methods).

IoLR5 RNA is present in the unfertilized egg, is localized to the centrosomes at the 2-cell and 4-cell stages, and then segregates into the first quartet cells (Kingsley et al., 2007) (as summarized in Fig. 1). At 16.5 hours after egg laying (AEL) (~70 cells), the transcript was abundant in $1a^{121}$, $1b^{121}$ and $1c^{121}$ (Fig. 1E and see Fig. S1 in

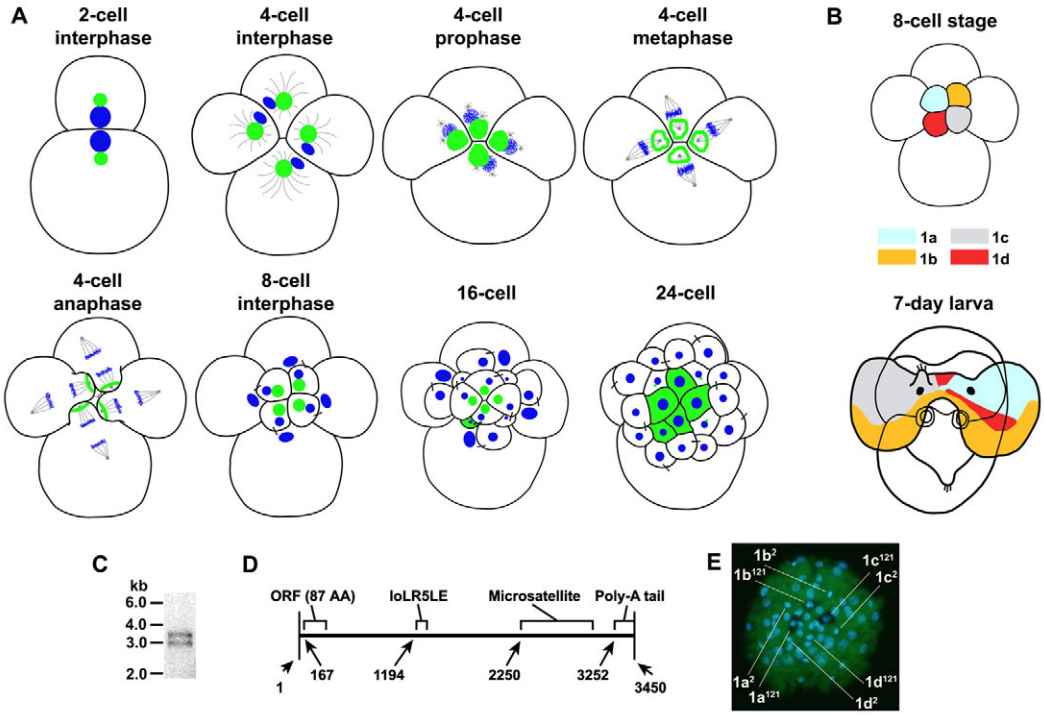

Fig. 1. IoLR5 mRNA localization and segregation during early cleavage stages of the *Ilyanassa* embryo. (**A**) IoLR5 mRNA distribution from 2-cell interphase to the 24-cell stage. RNA is green, DNA is blue and microtubules are gray. The RNA is localized on the centrosomes during 2-cell stage interphase and again at 4-cell stage interphase. During prophase, the transcript moves to the cortex above the nuclei where it flattens into a disc-shaped plaque. In metaphase, the spindle pole orients perpendicular to the RNA plaque and a hole appears in the RNA where the spindle pole approaches the cortex. At the 8-cell stage, the RNA is only found on the centrosomes of the first quartet. At the 16-cell stage, the RNA is on the centrosomes in $1q^1$, and is also diffuse in the cytoplasm of $1d^2$. At the 24-cell stage, the RNA is cytoplasmic in $1q^1$ and $1d^2$, and is weakly expressed in $1a^2$, $1b^2$ and $1c^2$, where it is localized to the centrosomes. Animal pole is towards the viewer and the D quadrant is down. Hatch marks show sister cells. (**B**) The first quartet micromeres give rise to head ectoderm and the contribution from each micromere (1a, 1b, 1c and 1d) is shown on an anterior view of a 7-day old larva. (**C**) Early cleavage RNA probed with IoLR5 identifies bands at ~3.0 and ~3.5 kb. (**D**) Full-length IoLR5 transcript. (**E**) At ~16.5 hours AEL, IoLR5 mRNA is abundant in $1a^{121}$, $1b^{121}$ and $1c^{121}$. Chromogenic staining of the RNA is observed as dark shadowing against a green background; nuclei are stained with DAPI (blue). For the identities of other cells, see Fig. S1 in the supplementary material.

the supplementary material). The RNA was found transiently in $1d^{121}$ progeny and appeared to become more abundant in the four trochoblast cells ($1q^2$, the main cells of the ciliated band); these observations suggest that there is zygotic IoLR5 transcription, at least in these lineages (Fig. 2A). At ~2 days AEL, IoLR5 mRNA was detected in two B quadrant cells at the ventral end of the apical plate and in groups of four cells on the left and right sides of the head that were derived from $1a^{121}$ and $1c^{121}$, respectively (Fig. 2C). A time course from 24 to 48 hours AEL showed that the IoLR5-expressing cells (Fig. 2C) were the descendants of $1a^{121}$, $1b^{121}$ and $1c^{121}$ (not shown). At 3 days AEL, these two groups of cells continued to divide and RNA was also observed in one cell on each side that was located dorsal to these clusters. The mRNA signal became increasingly weak and variable and by 4-5 days AEL the IoLR5 mRNA was no longer detectable by in situ hybridization.

IoLR5 protein distribution

Although the IoLR5 transcript is 3450 bases long, there is only one open reading frame (ORF) longer than 50 codons, which encodes a protein of 87 amino acids and has a strong translational start sequence (Fig. 1D) (Kozak, 1987). This protein has no significant homology to known proteins as assessed by BLAST searches of database sequences (Altschul et al., 1990). We raised and validated an anti-IoLR5 antibody (see Materials and methods) and examined expression by western blots. The protein was first detected at 24 hours AEL, peaked at 2 days AEL and began to decline by 4 days AEL, until it was no longer detectable on the western blot after 6 days AEL.

Whole-mount staining showed that IoLR5 protein is in the same cells as the RNA at 1-2 days AEL and persists after the RNA is no longer detectable, allowing us to follow the fates of IoLR5-expressing cells into organogenesis (Fig. 2B,D). The bilaterally paired dorsal IoLR5 cells do not divide in the interval that we examined (to 7 days AEL). These cells are located directly above the eyes (once these structures appear), in regions that are likely to develop into the tentacles. The paired ventral IoLR5-expressing cells also do not divide in this interval, and they become the ventral-most cells of the apical plate, the region of large cells in the middle of the developing head. The ventral and dorsal pairs of cells both maintained IoLR5 protein expression through 5.5 days AEL. Unlike the dorsal and ventral pairs of cells, each lateral cluster continues to divide and by 3 days AEL, nine IoLR5-expressing cells were apparent on each side (Fig. 2E,E′). By 4.5 days AEL, each cluster of nine cells had split such that the ventral portion (4-5 cells) was a few cell diameters from the dorsal group on each side (Fig. 2F,F′). Around 5-6 days AEL, the ventral group of cells was completely internal and was part of a densely packed mass of cells that form the cerebral ganglion. Only a subset of the dorsal group

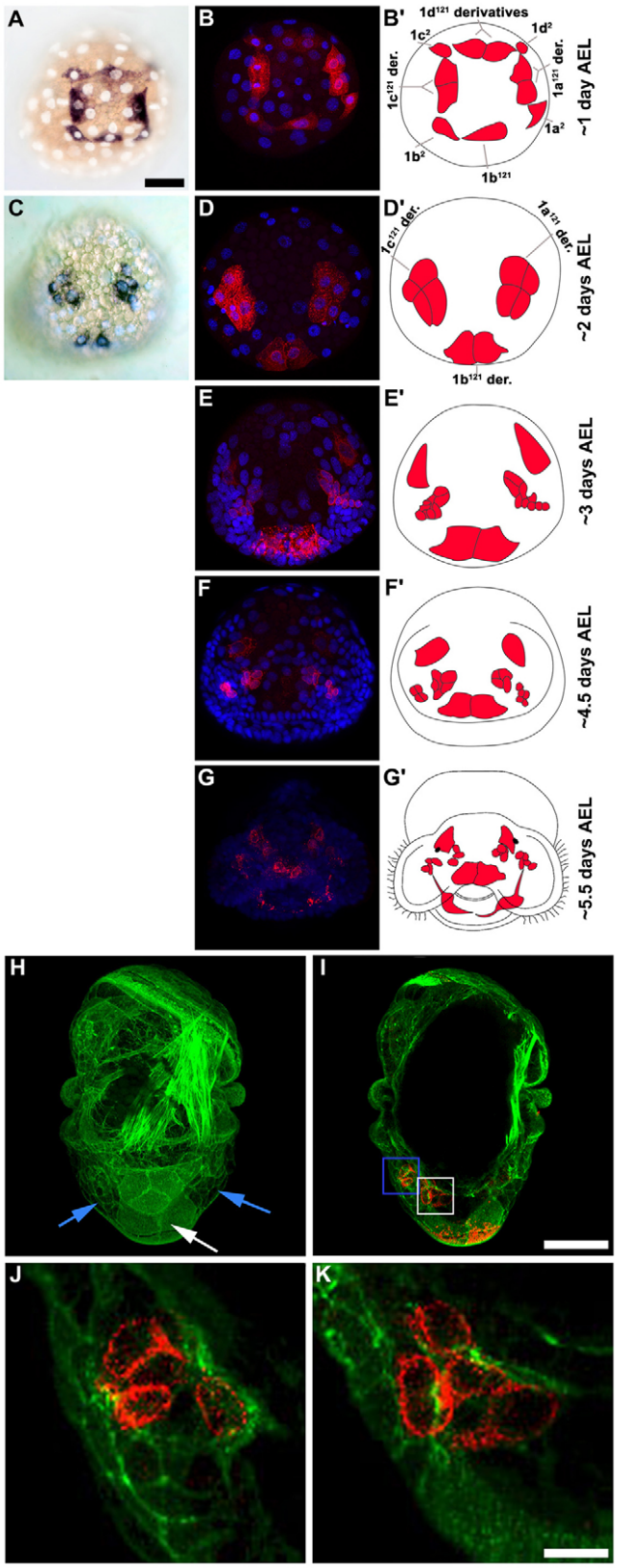

Fig. 2. Late stage IoLR5 mRNA and protein expression. (**A-G′**) The animal pole is towards the viewer and the D quadrant (dorsal side) is up. Schematic interpretations of the expression patterns are shown alongside (B′,D′,E′-G′). (A) In situ hybridization on ~1 day AEL *Ilyanassa* embryos shows that IoLR5 mRNA is expressed in $1q^{121}$ and $1q^{2}$. RNA staining is blue-black and nuclei are blue (DAPI). (B) Anti-IoLR5 protein staining at a stage slightly later than in A, when $1a^{121}$, $1c^{121}$ and $1d^{121}$ have divided. Antibody staining is red, nuclear DAPI staining is blue. (C,D) About 2 days AEL, mRNA expression (C) and protein expression (D) are lost in $1q^{2}$ and the D quadrant descendants, but remain in the A, B and C quadrants. (E) By 3 days AEL, the clusters in the A and C quadrants have nine cells each. Two cells dorsal to these clusters also have IoLR5 expression. (F) Anti-IoLR5 staining ~4.5 days AEL, showing the separation of the A and C quadrant clusters into two groups of cells in each. (G) Antibody staining at the early veliger stage shows internalized cells in the A and C quadrant clusters and neuronal processes. (**H-K**) Dorsal views of a ~4.5 day AEL embryo stained with the IoLR5 antibody (red) and phalloidin (green); anterior is down. (H) Projection of sections of phalloidin staining showing the apical plate (white arrow) and the regions where the cerebral ganglia will form (blue arrows). (I) A merged projection of a subset of sections showing the two clusters of the C quadrant lineage that are internalized. (J) Magnification of the blue boxed region in I. (K) Magnification of the white boxed region in I. Scale bars: 100 μm in A; 50 μm in I; 10 μm in K.

of cells was internalized. These cells also appeared to join the growing cerebral ganglion, while the remaining cells stayed on the velar surface ventral to the developing eye, until at least 7 days AEL (Fig. 2H-K). IoLR5 staining was also observed in two long processes that extend from the cerebral ganglia into the distal region of the foot (Fig. 2G,G′). These processes included at least two cell bodies, and appeared to be axons. Indeed, they are in the location reported for the pedal connectives (Dickinson and Croll, 2003). These results show that IoLR5-expressing cells generate several regions of head ectoderm and provide a major contribution to the cerebral ganglion, suggesting that IoLR5 is involved in the development of the nervous system in the head.

Phenotypic effects of IoLR5 knockdown

To determine the functional role of IoLR5 we injected a translation-blocking antisense morpholino oligonucleotide (IoLR5MO1) into zygotes and reared embryos to the veliger stage. Injection of IoLR5MO1 resulted in reproducible, dose-dependent phenotypes in the larvae. At 0.25 mM, there was no visible effect on development and at 1.5 mM or higher all animals arrested during, or immediately after, gastrulation (not shown). At 0.5 to 1 mM, animals suffered increasingly frequent defects in the velar lobes and eyes (head structures; Fig. 3). Less frequent defects in such tissues as the larval retractor muscle, intestine and statocysts were seen at similar levels across the range of concentrations (Fig. 3G, Table 1). Animals injected with a 1 mM Standard Control MO always exhibited wild-type development.

The eye phenotypes consisted of no eyes, one eye, or synopthalmia (in which the eyes are abnormally close; Fig. 3A-E′). At 1 mM IoLR5MO1, 86% (n=22) lacked one or both eyes and 95% had some kind of eye defect when synopthalmia was included. Surprisingly, injected animals that had only one eye were about three times more likely to be missing the right eye than the left (Table 1). These defects are very similar to those observed after ablation of first quartet cells. For instance, ablation of 1b causes synopthalmia, and ablation of 1a or 1c causes a smaller velar lobe or the lack of an eye on the left or right side, respectively (Clement, 1967).

Two lines of evidence indicate that the IoLR5MO1 phenotype is the result of a specific knockdown of IoLR5 translation. First, on western blots, the IoLR5 protein in IoLR5MO1-injected animals

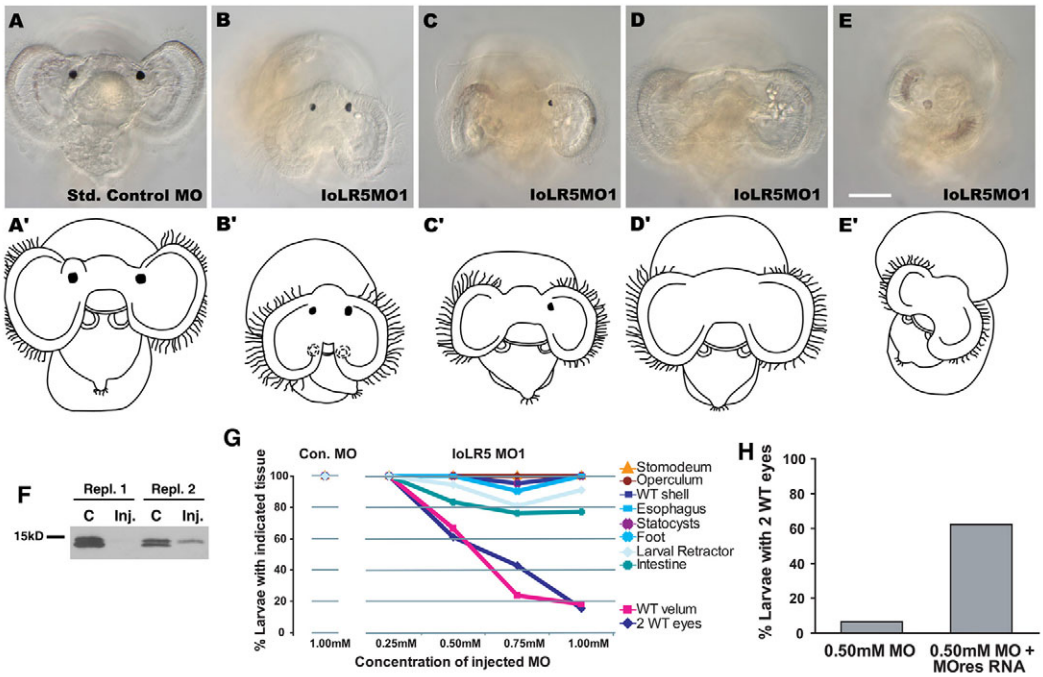

Fig. 3. Knockdown of IoLR5 by injection of IoLR5MO1. (**A**) Wild-type *Ilyanassa* larva from a zygote injected with the Standard Control MO. (**B-E**) Animals injected with IoLR5MO1 developed with several head defects including synopthalmia (B), one eye (C), no eyes (D), and small velar lobes with no eyes (E). Anterior views with dorsal up. Scale bar: 100 μm. (**A′-E′**) Schematic interpretations of the structures shown above. (**F**) Two replicates of a western blot analysis show that IoLR5 protein levels are reduced in IoLR5MO1-injected animals. For replicate 1, each lane contained protein from 47 embryos, both lanes from the same capsule. For replicate 2, each lane contained protein from 25 embryos from each of two capsules. The higher band might be post-translationally modified IoLR5 protein. (**G**) The percentage of animals with the indicated tissue for each concentration of injected morpholino (for scoring data see Table 1). (**H**) Rescue of the morpholino phenotype with IoLR5MOres RNA. After IoLR5MO1 injection, 5/80 larvae (6%) developed two wild-type eyes, but with co-injection with the IoLR5MOres mRNA 98/157 (62%) developed two wild-type eyes.

was either completely absent or strongly diminished compared with control animals (Fig. 3F). Second, the eye phenotypes were largely rescued when IoLR5MO1 was injected together with an IoLR5 mRNA that included seven mismatches in the morpholino target site (IoLR5MOres). In this experiment, 6% of IoLR5MO1-injected animals had two wild-type eyes (n=80), but when IoLR5MOres was co-injected with IoLR5MO1, 62% of the animals developed two wild-type eyes (n=157) (Fig. 3H). Injection of IoLR5MOres by itself had no effect on development and none of the rescue animals developed more than two eyes (not shown), indicating that the transcript is not sufficient for ectopic eye development.

Segregation of IoLR5 RNA requires centrosomal localization

Having shown that IoLR5 RNA is required for the development of first quartet derivatives, we turned to the question of how it is specifically segregated to these lineages. We first addressed whether centrosomal localization per se is required for asymmetric segregation by examining the fate of RNAs when centrosomal localization was bypassed.

We found that localization did not occur if RNA was injected after the interval when localization normally occurs. Preliminary experiments showed that an in vitro synthesized RNA

Table 1. Percentage of animals with wild-type development of the indicated larval organs

Conc. (mM)	Eyes†			Velum	Stomodeum	Foot	Two statocysts	Operculum	Shell	Esophagus‡	Intestine‡	Retractor muscle‡	Style sac‡	Stomach‡	Digestive gland‡
	Two eyes	Left only	Right only												
Standard Control MO															
1	100	0	0	100	100	100	100	100	100	100	100	100	100	100	100
IoLR5 MO1															
0.25	100	0	0	100	100	100	100	100	100	100	100	100	100	100	100
0.5	61	17	0	67	100	100	100	100	100	100	83	94	56	56	94
0.75	43*	29	10	24	100	90	95	100	95	90	76	81	48	38	57
1	14*	45	18	18	100	100	100	100	100	100	77	91	50	55	32

For the Standard Control MO, n=20; for the IoLR5 MO1, n=18 (0.25 and 0.5 mM), n=21 (0.75 mM) and n=22 (1 mM).
*These percentages include one animal with synopthalmia at 0.75 mM and two animals at 1 mM.
†Eyes that were only partially formed (small patches of pigment) were not counted as wild-type and account for the missing eye percentages for the 0.5, 0.75 and 1 mM IoLR5MO1 injections.
‡These structures were not always reliably scored owing to the presence of yolk within the shell (see Fig. S2 in the supplementary material).

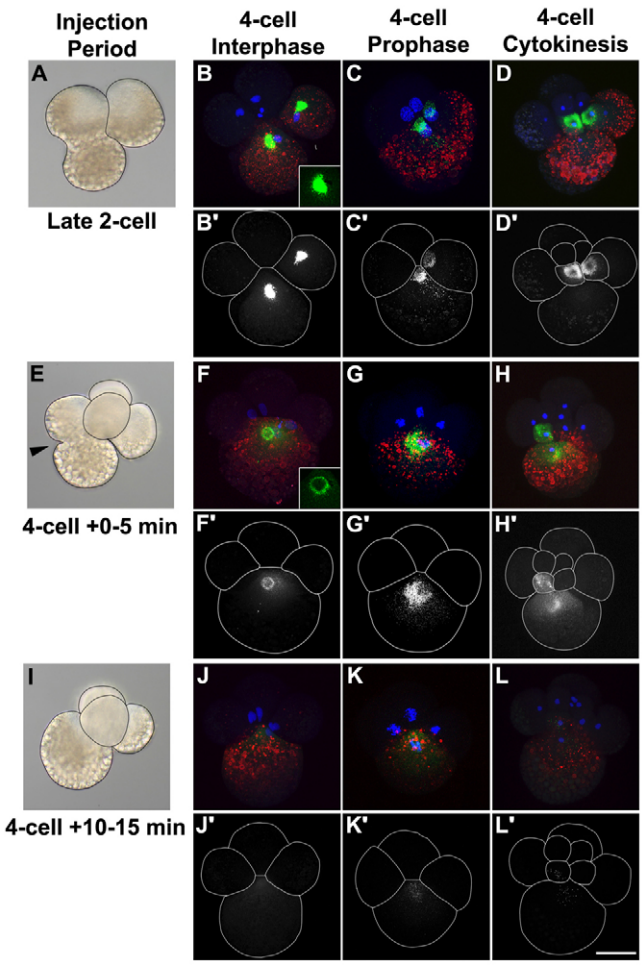

Fig. 4. Centrosomal localization is required for asymmetric segregation of IoLR5. (**A**) Two-cell stage *Ilyanassa* embryo (lateral view). (**B**) When IoLR5 RNA was injected at the 2-cell stage, as determined by the presence of the lineage tracer Sulforhodamine 101 (red) in two macromeres, the RNA (green) was later localized to the centrosomes during 4-cell stage interphase. DNA is blue (DAPI). Projections of confocal *z*-stacks; the inset shows a single section through the centrosome. (**C**,**D**) The IoLR5 RNA is on the cortex at prophase (C) and segregated to the micromeres during cytokinesis (D). (**E**) The first 5 minutes of the 4-cell stage (4-cell + 0-5 min) are characterized by the presence of a constriction in the large D cell (arrowhead). (**F**) When IoLR5 RNA is injected during this interval, localization is to the surface of the interphase centrosome (inset shows a single section through the centrosome). (**G**) IoLR5 RNA then moves as speckles to the cortex in prophase. (**H**) A portion of the detectable IoLR5 RNA in the mother cell is segregated to the micromere daughter. (**I**) Ten minutes after the start of the 4-cell stage, the constriction of D is no longer present. (**J-L**) Injections 10-15 minutes into the 4-cell stage (4-cell + 10-15 min) result in no centrosomal localization (J), or cortical localization (K), or segregation (L). In I-L, the injected RNA is still present, but difficult to image when it is diffuse in the cytoplasm (see Fig. S3 in the supplementary material). A, E and I are lateral views; the remainder are from the animal pole. (**B′-D′**,**F′-H′**,**J′-L′**) RNA alone. Scale bar: 100 μm.

corresponding to bases 1-2055 of IoLR5 and labeled with Alexa Fluor 488 could recapitulate localization to 4-cell stage centrosomes and segregation to the first quartet micromeres when it was injected into the zygote. To examine whether later-injected RNA would also be localized, the RNA was injected at various time points from late 2-cell stage until 15 minutes into the 4-cell stage. RNA localization was examined every 10 minutes until the mid 8-cell stage, to ensure that only embryos with normal division were included in the analysis. Embryos with representative staining patterns were fixed, stained and imaged by confocal microscopy. When RNA was injected during the 2-cell stage, it always localized to the centrosome (*n*=16; Fig. 4A,B). Of the embryos injected after the end of cytokinesis, around half (14/30) had a strikingly different pattern of localization, in which RNAs localized to a shallow zone on the surface of the centrosome (Fig. 4F). The remainder of the injections in this class showed no localization (16/30; Fig. 4J). To determine whether these two patterns were related to the timing of injection, we performed additional injections that were staged based on the distinct morphology of the embryo in the first 5 minutes of the 4-cell stage (Fig. 4E). We found that the majority (21/24) of injections in this interval showed localization to the surface of the centrosome (as in Fig. 4F), with the remainder showing no localization (as in Fig. 4J), and that injections 10 minutes later showed no localization (*n*=33). The shallow localization suggests that the RNA-containing pericentriolar matrix accumulates progressively on the outside surface of the centrosome, with minimal mixing. The presence of both shallow localization and no localization in the embryos injected during the first 5 minutes of the 4-cell stage indicates that transport to the centrosome ends during this interval.

To evaluate the importance of centrosomal localization for subsequent RNA segregation, we followed the behavior of injected RNAs later in the cell cycle. When RNA did localize to the centrosome it moved to the cortex during prophase and was predominantly asymmetrically segregated into the first quartet micromeres, as observed for IoLR5 RNA injected into zygotes (Fig. 4C-D′). When shallow localization was observed (as in 4-cell + 0-5 min injections), the labeled RNA moved to the cortex as above but as individual speckles of signal, and only a portion of the RNA was segregated (Fig. 4G-H′). When RNA did not localize during interphase (as in 4-cell + 10-15 min), it did not move to the cortex at prophase and was not segregated asymmetrically (Fig. 4K-L′); instead, the RNA remained cytoplasmic until the next interval, when it localized to the micromere and macromere centrosomes at 8-cell stage interphase. This demonstrates that the RNAs remain competent to localize even if they miss the window for transport at the third cleavage (see Fig. 7 and Fig. S3 in the supplementary material).

It might be that segregation requires an event that is concurrent with centrosomal localization but not dependent on it, but this seems less probable than a model in which localization to the centrosome per se is required for RNA segregation. The centrosome could be the site of an essential processing or packaging event, or it might be that the transport only occurs when RNAs are anchored to the pericentriolar matrix material.

The IoLR5 localization element

The large number of RNA localization and segregation patterns in the *Ilyanassa* embryo suggests that this system is under very intricate control. One way that this could be generated is by specific RNA localization elements (LEs) (see Martin and Ephrussi, 2009; St Johnston, 2005). To test whether RNA segregation in *Ilyanassa* relies on an LE, we adapted the fluorescence assay described above to map regions involved in centrosomal localization. Digoxigenin-labeled RNA corresponding to the original clone (bp 1-2055) could recapitulate centrosomal

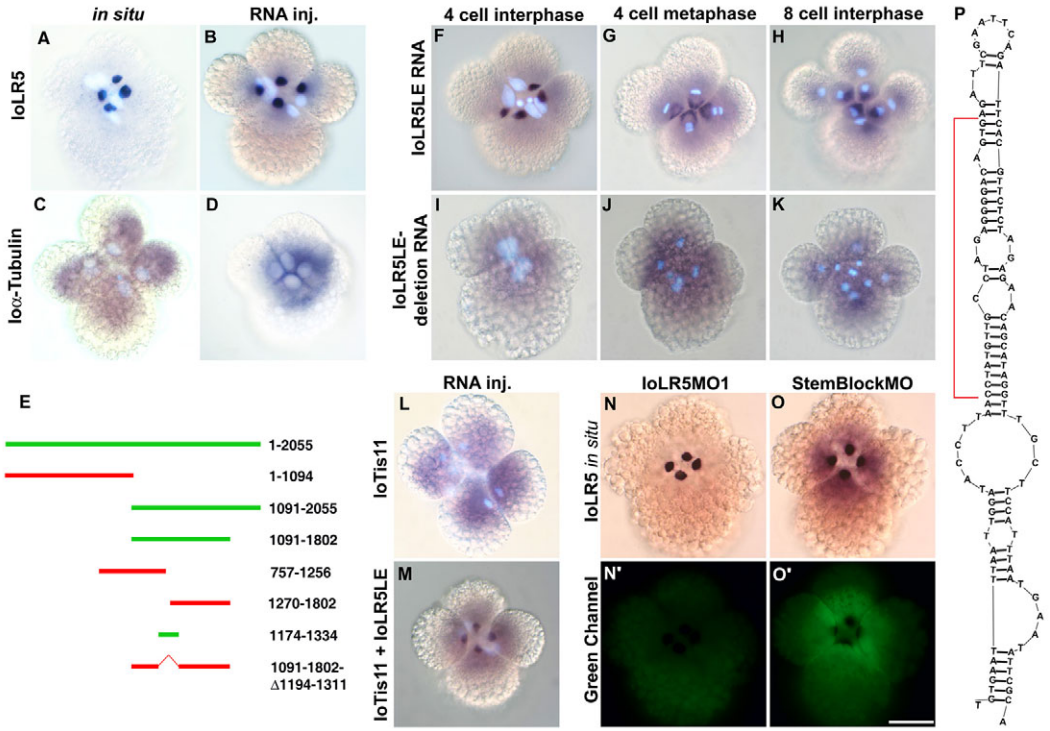

Fig. 5. Mapping the IoLR5 localization element (LE). (**A**,**C**) In situ hybridization shows that IoLR5 mRNA is localized to the centrosomes at 4-cell interphase (A), whereas the control IoAlpha-Tubulin mRNA is cytoplasmic (C). (**B**,**D**) An RNA transcribed in vitro, corresponding to bases 1-2055 of IoLR5 and labeled with digoxigenin-UTP, was injected into zygotes and localized to centrosomes at 4-cell interphase (B), whereas a labeled IoAlpha-Tubulin mRNA remained cytoplasmic (D). (**E**) Regions of the IoLR5 transcript that localized are in green and regions that did not are in red. (**F-H**) The labeled IoLR5LE RNA is able to localize to the centrosomes at the 4-cell stage (F), to the cortex during metaphase (G), and is mainly segregated into the first quartet after cytokinesis (H). Some of the injected RNA was not segregated and is on the centrosomes in the macromeres (out of the plane of focus). (**I-K**) A region of IoLR5 with the LE bases deleted (1091-1802) was unable to localize to the centrosome (I), or cortex (J), and was not asymmetrically segregated (K). (**L**) A labeled IoTis11 transcript does not localize to 4-cell stage centrosomes. (**M**) Insertion of the IoLR5LE was sufficient to localize IoTis11 RNA at the 4-cell stage. (**N-O'**) *Ilyanassa* embryos from the same capsule were injected with either the IoLR5MO1 and a red lineage tracer (N,N') or a morpholino designed to block the center of the LE (StemBlockMO; target site is bracketed in P) with a green fluorescent lineage tracer (O,O'). Embryos were pooled and processed together to allow qualitative comparison of localization, and then sorted based on fluorescent lineage tracers. Injection of StemBlockMO impaired localization, but the translation-blocking morpholino did not. (**P**) The smallest region capable of being transported to the centrosome (1174-1334) is predicted to form a single large stem-loop secondary structure from bases 1194-1312 (IoLR5LE). Scale bar: 100 μm.

localization after injection into zygotes (compare Fig. 5B with 5A), whereas an antisense transcript of IoLR5 bases 1-2055 failed to localize (not shown). Labeled IoAlpha-Tubulin mRNA did not localize, consistent with its endogenous transcript (Fig. 5C,D). Together, these results show that this approach is effective and specific.

We mapped the localization activity of the original clone by testing various fragments, and found that localization required a region around base 1260 (Fig. 5E). In silico folding of the entire IoLR5 RNA with RNAstructure 4.6 (Mathews, 2006) predicted a large, 118-base stem-loop at bases 1194-1312 (Fig. 5P). This structure was assigned the highest probability of any in the sequence, and was the only structure found in each of the top 20 secondary structure predictions, suggesting that the 118-base stem-loop is likely to be present in vivo. We tested this small fragment and discovered that it localizes to the centrosome (Fig. 5F). We then deleted this 118-base region from IoLR5(1091-1802) and this caused the RNA to remain distributed throughout the cytoplasm (Fig. 5I). These results demonstrate that this region is necessary for the localization of IoLR5 to 4-cell centrosomes and is sufficient to localize itself. To test whether the predicted secondary structure is sufficient to localize a normally unlocalized RNA, we inserted the stem-loop structure into the IoTis11 RNA, which does not normally localize to 4-cell stage centrosomes (Kingsley et al., 2007) (Fig. 5L). The resulting RNA localized to 4-cell stage centrosomes, demonstrating that the stem-loop is sufficient to confer localization (Fig. 5L,M). We refer to this 118-base region as the IoLR5LE.

To examine whether the proper secondary structure of the LE is important for its role as a centrosomal localization signal, we took advantage of the fact that morpholinos can be used to disrupt RNA secondary structure [e.g. in splicing or miRNA biogenesis (Draper et al., 2001; Kloosterman et al., 2007)]. We designed a morpholino targeted to a region near the center of the IoLR5LE stem-loop (IoLR5StemBlockMO; Fig. 5P). Injection of this molecule into zygotes caused a significant impairment of localization of the endogenous IoLR5 transcript (Fig. 5O), whereas injection of the translation-blocking morpholino did not affect localization (Fig. 5N). This novel approach suggests that the secondary structure of the IoLR5LE is important for centrosomal localization. Despite the partial inhibition of centrosomal localization at the 4-cell stage, these animals still developed into apparently wild-type veligers.

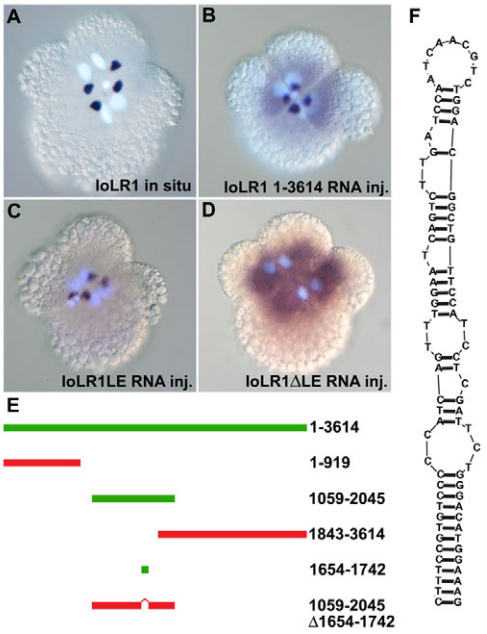

Fig. 6. Mapping the LE for another 4-cell-localized RNA, IoLR1. (**A**) In situ hybridization of IoLR1 RNA on the centrosomes at the 4-cell stage. (**B**) A digoxigenin-labeled transcript corresponding to the original cDNA clone for IoLR1 (bases 1-3614) localized at the 4-cell stage. (**C**) The smallest region that we found that was capable of localization was IoLR1(1654-1742). (**D**) When this region was deleted, the transcript failed to localize. (**E**) Tested regions of the IoLR1 transcript that localized are shown in green and regions that did not are in red. (**F**) The predicted secondary structure of the IoLR1LE.

We followed the behaviors of the LE and deletion constructs after centrosomal localization. The IoLR5LE localized to the cortex during prophase and was asymmetrically segregated into the 8-cell stage micromeres (Fig. 5F-H). By contrast, the LE deletion transcript remained cytoplasmic throughout the 4-cell stage and was never asymmetrically segregated (Fig. 5I-K). These data demonstrate that the IoLR5LE is necessary for all phases of the segregation process. Although the IoLR5LE was capable of recapitulating the movements of the endogenous RNA, it did so with decreased specificity. When the endogenous RNA segregates during 4-cell stage cytokinesis, all of the transcripts are delivered to the first quartet and none is detectable in the macromeres. For the injected RNAs, centrosome localization during interphase was very specific; however, not all of the injected transcripts became asymmetrically segregated as some were still visible in the macromeres at the 8-cell stage (see Fig. 5H, Fig. 7 and see Fig. S3 in the supplementary material).

Another first quartet RNA requires an element with a similar secondary structure to IoLR5LE for localization

During the third cleavage, the IoLR1 RNA is temporally and spatially coincident with IoLR5 (Kingsley et al., 2007). The original cDNA clone was 3.6 kb and the complete transcript is ~9.6 kb, based on northern blotting (not shown). We tested several fragments of the original 3.6 kb clone for localization to 4-cell stage centrosomes (Fig. 6A-C,E) and found a 1 kb region that could localize. We folded this fragment using RNAstructure 4.6 and three large stem-loops were found to be highly probable. Each of these was individually tested for 4-cell localization, but only one localized (Fig. 6C,E,F). When this region was deleted from the 1 kb fragment, centrosomal localization was abolished (Fig. 6D), showing that this 88-base sequence is necessary for localization of IoLR1. We refer to this region as the IoLR1LE.

We attempted to test whether the two LEs use the same machinery through competition experiments. However, we were unable to competitively inhibit centrosomal localization of either endogenous or exogenous IoLR5 RNA, even at a 1000-fold molar excess of injected IoLR5LE RNA (not shown). We were also unable to competitively inhibit localization of other first quartet RNAs with IoLR5LE. These results suggest that the centrosomal transport machinery is not limiting during the localization process.

Localization of LEs at other stages of development

We have focused on the control of localization at the 4-cell stage, but examination of the behavior of LEs at other stages is informative regarding how the specificity and complexity of localization are achieved. The endogenous IoLR5 and IoLR1 RNAs are both localized to centrosomes at the 4-cell stage, but at the 2-cell stage only IoLR5 is localized to the centrosomes (Kingsley et al., 2007). We mapped the sequences required for centrosomal localization of IoLR5 at the 2-cell stage, and found that this required the same region as for 4-cell localization, i.e. IoLR5LE (Fig. 7A,B). We next tested 2-cell stage localization for IoLR1(1059-2045), which contains the LE for 4-cell stage localization. Surprisingly, this injected RNA was occasionally capable of very weak localization at the 2-cell stage (Fig. 7C). Since the IoLR1 fragment only had weak and variable localization, we did not attempt fine-scale mapping for this region.

The endogenous IoLR5 and IoLR1 transcripts are highly specific for the first quartet and are not found in the second or third quartet micromeres. Since our injected RNAs were not completely segregated, we were able to follow injected RNAs later in development and test for localization in cells in which these messages are not normally found. We discovered that the injected RNAs can localize to macromere centrosomes at the 8-cell stage (Fig. 7D,E). Furthermore, at the 24-cell stage, when the first, second and third quartets are all present, the injected RNAs were centrosomally localized in all cells of the embryo (Fig. 7F,G), even though the endogenous RNAs are never observed in many of these cells. Similarly, the IoLR5LE RNA was centrosomally localized in the $1q^1$ cells at the 24-cell stage, even though the endogenous message is always cytoplasmic at this stage. The injected RNAs were not appreciably degraded, which might be important for establishing the normal pattern of endogenous transcripts. These results indicate that transcript abundance is tightly regulated to ensure the proper distribution of segregated RNAs and they hint that other mechanisms are in place that can prevent transcript localization, even when an LE is present.

DISCUSSION

One of the hallmarks of spiralian development is the patterning of the animal-vegetal axis by the production of tiers of cells, called quartets, with different developmental potentials, but the mechanisms that control this are unknown. Our results show that a segregated RNA is functionally important for quartet-specific developmental potential. The IoLR5 mRNA is specifically segregated into the first quartet of micromeres, which generate the larval head. Inhibiting IoLR5 translation impairs the development of larval head structures, particularly the eyes and velum,

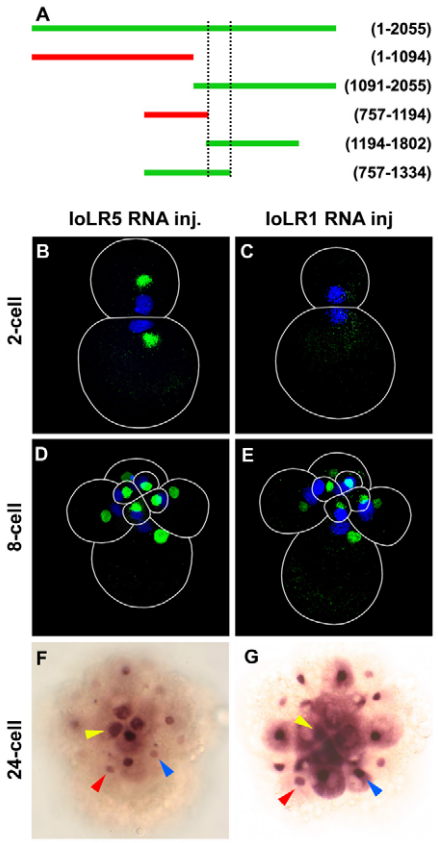

Fig. 7. IoLR5 and IoLR1 localization at the 2-, 8- and 24-cell stages. (**A**) Using fluorescently labeled segments of IoLR5 RNA, we mapped the region required for centrosomal localization at the 2-cell stage. Green bars represent regions that localized and red bars indicate regions that did not localize; dotted lines indicate the inferred required region. Two-cell localization could not be mapped with digoxigenin-labeled RNAs or RNAs that were shorter than 500 bases (see Materials and methods). (**B**) Projection of confocal *z*-stack showing centrosomal localization of fluorescently labeled IoLR5(1194-1802). RNA is green, DNA (DAPI) is blue. (**C**) A fragment of IoLR1(1059-2045) containing the 4-cell LE was able to localize to 2-cell centrosomes, but this was only observed occasionally and was very weak. (**D**,**E**) At the 8-cell stage, IoLR5(1194-1802) (D) and IoLR1(1059-2045) (E) were localized in the first quartet micromeres, as well as in the macromeres. (**F**,**G**) At the 24-cell stage, IoLR5LE (F) and IoLR1(1059-2045) (G) RNAs were localized in the first quartet micromeres (yellow arrowheads show $1a^1$), the second quartet micromeres (blue arrowheads show $2d^2$) and the third quartet micromeres (red arrowheads show 3d). Although fluorescent RNAs showed the same pattern of 24-cell localization, digoxigenin-labeled RNAs were used here because they better show the level of injected RNA in the cytoplasm.

demonstrating the functional role of the protein in development. There is no IoLR5 expression in the cells that become the eyes, indicating that the effect is non-cell-autonomous. The eyes develop in the optic ganglia, which arise in contact with the cerebral ganglia where IoLR5 protein is found (Gibson, 1984; Lin and Leise, 1996). Thus, our results suggest that the proper development of the eyes or optic ganglia might require previously unappreciated signaling cues from proneural or neural tissues.

Our experiments suggest a model of how first quartet-specific localization arises. We characterized an RNA element that mediates localization to the centrosome at the 4-cell stage and segregation to the first quartet. We found a similar element in another RNA that is segregated to the first quartet, and we propose that these two elements define a class of RNA sequences that mediate localization to the first quartet and thus contribute to first quartet identity. These elements are also capable of mediating segregation of injected RNAs to other quartets, even though the endogenous messages are only segregated into the first quartet. Thus, our data indicate that specific first quartet localization is achieved by ensuring that no significant population of a first quartet RNA molecule remains in the macromeres to be segregated in the next mitosis. This seems to be achieved by highly efficient transport mechanisms and, in some cases, by RNA decay. The high capacity and efficiency of this transport are supported by several lines of evidence. First, for most first quartet RNAs, such as IoLR5 and IoLR1, we cannot detect any RNA in the macromeres immediately following division. Second, we have found that centrosomal localization can occur as late as 5 minutes after the beginning of the 4-cell stage, but that endogenous IoLR5 and IoLR1 RNAs are localized well before this, during cytokinesis (see Kingsley et al., 2007). Finally, we attempted to saturate the transport machinery by injecting high molar excesses of IoLR5LE RNA, but were unable to competitively inhibit endogenous IoLR5 or IoLR1 RNA, or injected IoLR1 RNA, from localizing to the centrosome. RNA decay also appears to play a role in maintaining quartet specificity. In the case of IoEve mRNA, which is segregated to the first quartet, a fraction of RNAs remain in the macromeres, and first quartet specificity is achieved by decay of the message in the macromeres (Lambert and Nagy, 2002). Thus, first quartet-specific segregation appears to be controlled by a combination of specific RNA secondary structures and regulation of transcript abundance.

A number of aspects of RNA localization in the early *Ilyanassa* embryo remain unclear. We do not understand why our injected RNAs can perfectly recapitulate the specificity of centrosomal localization, but are less specific later in the cell cycle and during segregation. We also do not understand how the transition to cytoplasmic distribution is controlled: injected IoLR5 is centrosomal in the $1q^1$ cells at the 24-cell stage, but endogenous IoLR5 is cytoplasmic in these cells. Finally, despite the fact that we have identified sequence elements that will segregate into the second and third quartets, we do not know how localization to other quartets occurs. We have injected putatively full-length RNAs for several transcripts that are segregated to the second and third quartets and never observed localization (our unpublished results), suggesting that the mechanism used is different from that employed during first quartet localization.

For the localized RNAs that have been characterized in other organisms, such as *bicoid*, *oskar* and *Vg1*, translation is typically required soon after localization or fertilization of the oocyte (Kugler and Lasko, 2009; Martin and Ephrussi, 2009; St Johnston, 2005). The IoLR5 mRNA is asymmetrically segregated very early during embryogenesis, during the third cleavage, and it is reiteratively segregated through several more rounds of divisions to the $1q^{121}$ cells, before the protein is detectable. The protein is maintained in these cell lineages for several days and is eventually expressed in differentiated neurons; it is also required for development of the eyes, which form relatively late in organogenesis. The long interval of progressive segregation is striking. It suggests that for at least some factors, very fine-scale patterning is achieved by sequential segregation, rather than by a

hierarchical network of patterning factors that progressively subdivide the embryo, as observed frequently in somatic patterning of other systems. Although it is uncommon for somatic RNAs to be regulated in this manner during embryogenesis, with the exception of several RNAs studied in ascidian embryos (Nishida and Sawada, 2001), this mode of patterning is very common for germ plasm. In many organisms, components of the germ plasm are segregated through several rounds of cell division to the lineage that will form the germ line (Lehmann and Ephrussi, 1994; Seydoux and Schedl, 2001). This relationship to germ plasm is intriguing because the centrosome-mediated RNA localization seen in *Ilyanassa* might be homologous to a process observed in oogenesis across the animal kingdom – localization to the Balbiani body (Lambert, 2009). In *X. laevis*, *D. melanogaster* and *D. rerio*, RNAs and other cargoes localize to this structure during oogenesis before transport to the cortex, similar to the centrosomal RNAs in *Ilyanassa* (Cox and Spradling, 2003; Heinrich and Deshler, 2009; Kloc et al., 2004b; Marlow and Mullins, 2008). At least in frogs, in which the ultrastructure of the developing Balbiani body has been followed, it arises from the oocyte centrosome (Kloc et al., 2004a). We propose that *Ilyanassa* has extended this conserved patterning mechanism from the oocyte to early cleavage divisions.

This work raises the possibility that all spiralian embryos rely on centrosome-mediated RNA segregation to pattern the micromere quartets. Consistent with this, mRNAs of several putative patterning genes have been shown to be localized to centrosomes and then asymmetrically segregated in the snail *Crepidula fornicata* (Henry et al., 2010). Similarly, multiple RNAs are localized to the centrosomes in the surf clam *Spisula*, although this work did not follow the RNAs during cell divisions to see whether they are asymmetrically segregated (Alliegro et al., 2006). Given the strong conservation of the cell fates produced by spiralian micromere quartets, it seems likely that regulatory factors that generate these fates are also conserved across this group. As such factors are identified, it will be interesting to see how their quartet specificity is established in diverse spiralian embryos.

Acknowledgements
We thank Yingli Duan, Samantha Falk and Michael Cypress for technical assistance and Xin Yi Chan, Pamela Agbu and Hyla Sweet for comments on the manuscript. This work was supported by N.S.F. grants IOB-0544220 and IOB-0844734 to J.D.L.

Competing interests statement
The authors declare no competing financial interests.

Supplementary material
Supplementary material for this article is available at
http://dev.biologists.org/lookup/suppl/doi:10.1242/dev.055269/-/DC1

References

Ackermann, C., Dorresteijn, A. and Fischer, A. (2005). Clonal domains in postlarval *Platynereis dumerilii* (Annelida: Polychaeta). *J. Morphol.* **266**, 258-280.
Alliegro, M. C., Alliegro, M. A. and Palazzo, R. E. (2006). Centrosome-associated RNA in surf clam oocytes. *Proc. Natl. Acad. Sci. USA* **103**, 9034-9038.
Altschul, S. F., Gish, W., Miller, W., Myers, E. W. and Lipman, D. J. (1990). Basic local alignment search tool. *J. Mol. Biol.* **215**, 403-410.
Boyer, B. C., Henry, J. Q. and Martindale, M. Q. (1996). Dual origins of mesoderm in a basal spiralian: cell lineage analyses in the polyclad turbellarian Hoploplana inquilina. *Dev. Biol.* **179**, 329-338.
Clement, A. C. (1967). The embryonic value of micromeres in I*lyanassa obsoleta*, as determined by deletion experiment. I. The first quartet cells. *J. Exp. Zool.* **166**, 77-88.
Collier, J. R. (1981). Methods of obtaining and handling eggs and embryos of the marine mud snail *Ilyanassa obsoleta*. In *Laboratory Animal Management: Marine Invertebrates* (ed. National Resource Council U.S.), pp. 217-232. Washington DC: National Academy Press.
Cox, R. T. and Spradling, A. C. (2003). A Balbiani body and the fusome mediate mitochondrial inheritance during Drosophila oogenesis. *Development* **130**, 1579-1590.
Damen, P. and Dictus, W. J. (1994). Cell lineage of the prototroch of Patella vulgata (Gastropoda, Mollusca). *Dev. Biol.* **162**, 364-383.
Dickinson, A. J. G. and Croll, R. P. (2003). Development of the larval nervous system of the gastropod Ilyanassa obsoleta. *J. Comp. Neurol.* **466**, 197-218.
Draper, B. W., Morcos, P. A. and Kimmel, C. B. (2001). Inhibition of zebrafish fgf8 pre-mRNA splicing with morpholino oligos: a quantifiable method for gene knockdown. *Genesis* **30**, 154-156.
Dunn, C. W., Hejnol, A., Matus, D. Q., Pang, K., Browne, W. E., Smith, S. A., Seaver, E., Rouse, G. W., Obst, M., Edgecombe, G. D. et al. (2008). Broad phylogenomic sampling improves resolution of the animal tree of life. *Nature* **452**, 745-749.
Gharbiah, M., Cooley, J., Leise, E. M., Nakamoto, A., Rabinowitz, J. S., Lambert, J. D. and Nagy, L. M. (2009). The snail Ilyanassa: a reemerging model for studies in development. *CSH Protoc.* **2009**, pdb emo120.
Gibson, B. L. (1984). Cellular and ultrastructural features of the adult and the embryonic eye in the marine gastropod, Ilyanassa-Obsoleta. *J. Morphol.* **181**, 205-220.
Heinrich, B. and Deshler, J. O. (2009). RNA localization to the Balbiani body in Xenopus oocytes is regulated by the energy state of the cell and is facilitated by kinesin II. *RNA* **15**, 524-536.
Hejnol, A., Martindale, M. Q. and Henry, J. Q. (2007). High-resolution fate map of the snail Crepidula fornicata: the origins of ciliary bands, nervous system, and muscular elements. *Dev. Biol.* **305**, 63-76.
Henry, J. J. and Martindale, M. Q. (1998). Conservation of the spiralian developmental program: cell lineage of the nemertean, Cerebratulus lacteus. *Dev. Biol.* **201**, 253-269.
Henry, J. J. and Martindale, M. Q. (1999). Conservation and innovation in spiralian development. *Hydrobiologia* **402**, 255-265.
Henry, J. Q., Okusu, A. and Martindale, M. Q. (2004). The cell lineage of the polyplacophoran, Chaetopleura apiculata: variation in the spiralian program and implications for molluscan evolution. *Dev. Biol.* **272**, 145-160.
Henry, J. J., Perry, K. J., Fukui, L., and Alvi, N. (2010). Differential localization of mRNAs during early development in the mollusc, *Crepidula fornicata*. *Int. Comp. Biol.* **50**, 720-733.
Huang, F. Z., Kang, D., Ramirez-Weber, F. A., Bissen, S. T. and Weisblat, D. A. (2002). Micromere lineages in the glossiphoniid leech Helobdella. *Development* **129**, 719-732.
Kingsley, E. P., Chan, X. Y., Duan, Y. and Lambert, J. D. (2007). Widespread RNA segregation in a spiralian embryo. *Evol. Dev.* **9**, 527-539.
Kloc, M., Bilinski, S., Dougherty, M. T., Brey, E. M. and Etkin, L. D. (2004a). Formation, architecture and polarity of female germline cyst in *Xenopus*. *Dev. Biol.* **266**, 43-61.
Kloc, M., Bilinski, S. and Etkin, L. D. (2004b). The Balbiani body and germ cell determinants: 150 years later. *Curr. Top. Dev. Biol.* **59**, 1-36.
Kloosterman, W. P., Lagendijk, A. K., Ketting, R. F., Moulton, J. D. and Plasterk, R. H. (2007). Targeted inhibition of miRNA maturation with morpholinos reveals a role for miR-375 in pancreatic islet development. *PLoS Biol.* **5**, e203.
Kozak, M. (1987). An analysis of 5′-noncoding sequences from 699 vertebrate messenger RNAs. *Nucleic Acids Res.* **15**, 8125-8148.
Kugler, J. M. and Lasko, P. (2009). Localization, anchoring and translational control of oskar, gurken, bicoid and nanos mRNA during Drosophila oogenesis. *Fly (Austin)* **3**, 15-28.
Lambert, J. D. (2009). Patterning the Spiralian embryo: insights from Ilyanassa. *Curr. Top. Dev. Biol.* **86**, 107-133.
Lambert, J. D. (2010). Developmental patterns in spiralian embryos. *Curr. Biol.* **20**, R72-R77.
Lambert, J. D. and Nagy, L. M. (2001). MAPK signaling by the D quadrant embryonic organizer of the mollusc Ilyanassa obsoleta. *Development* **128**, 45-56.
Lambert, J. D. and Nagy, L. M. (2002). Asymmetric inheritance of centrosomally localized mRNAs during embryonic cleavages. *Nature* **420**, 682-686.
Lehmann, R. and Ephrussi, A. (1994). Germ plasm formation and germ cell determination in Drosophila. *Ciba Found. Symp.* **182**, 282-300.
Lin, M. F. and Leise, E. M. (1996). Gangliogenesis in the prosobranch gastropod Ilyanassa obsoleta. *J. Comp. Neurol.* **374**, 180-193.
Marlow, F. L. and Mullins, M. C. (2008). Bucky ball functions in Balbiani body assembly and animal-vegetal polarity in the oocyte and follicle cell layer in zebrafish. *Dev. Biol.* **321**, 40-50.
Martin, K. C. and Ephrussi, A. (2009). mRNA localization: gene expression in the spatial dimension. *Cell* **136**, 719-730.
Maslakova, S. A., Martindale, M. Q. and Norenburg, J. L. (2004). Fundamental properties of the spiralian developmental program are displayed by the basal

nemertean Carinoma tremaphoros (Palaeonemertea, Nemertea). *Dev. Biol.* **267**, 342-360.
Mathews, D. H. (2006). RNA secondary structure analysis using RNAstructure. *Curr. Protoc. Bioinformatics* **Chapter 12**, Unit 12.6.
Nishida, H. and Sawada, K. (2001). macho-1 encodes a localized mRNA in ascidian eggs that specifies muscle fate during embryogenesis. *Nature* **409**, 724-729.
Rabinowitz, J. S., Chan, X. Y., Kingsley, E. P., Duan, Y. and Lambert, J. D. (2008). Nanos is required in somatic blast cell lineages in the posterior of a mollusk embryo. *Curr. Biol.* **18**, 331-336.
Render, J. (1991). Fate maps of the first quartet micromeres in the gastropod Ilyanassa obsoleta. *Development* **113**, 495-501.
Render, J. (1997). Cell fate maps in the Ilyanassa obsoleta embryo beyond the third division. *Dev. Biol.* **189**, 301-310.
Schleip, W. (1929). *Die Determination der Primitiventwicklung*. Leipzig: Akad. Verlag.
Schneider, S. Q. and Bowerman, B. (2007). beta-catenin asymmetries after all animal/vegetal-oriented cell divisions in *Platynereis dumerilli* embryos mediate binary cell-fate specification. *Dev. Cell* **13**, 73-86.
Seydoux, G. and Schedl, T. (2001). The germline in C. elegans: origins, proliferation, and silencing. *Int. Rev. Cytol.* **203**, 139-185.
St Johnston, D. (2005). Moving messages: the intracellular localization of mRNAs. *Nat. Rev. Mol. Cell Biol.* **6**, 363-375.
Sweet, H. C. (1998). Specification of first quartet micromeres in Ilyanassa involves inherited factors and position with respect to the inducing D macromere. *Development* **125**, 4033-4044.
Szewczyk, E., Nayak, T., Oakley, C. E., Edgerton, H., Xiong, Y., Taheri-Talesh, N., Osmani, S. A. and Oakley, B. R. (2006). Fusion PCR and gene targeting in Aspergillus nidulans. *Nat. Protoc.* **1**, 3111-3120.
Weisblat, D. A. and Shankland, M. (1985). Cell lineage and segmentation in the leech. *Philos. Trans. R. Soc. Lond. B Biol. Sci.* **312**, 39-56.